

# New 4-Maleamic Acid and 4-Maleamide Peptidyl Chalcones as Potential Multitarget Drugs for Human Prostate Cancer

Juan Rodrigues • Claudia Abramjuk • Luis Vásquez • Neira Gamboa • José Domínguez • Bianca Nitzsche • Michael Höpfner • Radostina Georgieva • Hans Bäumlér • Carsten Stephan • Klaus Jung • Michael Lein • Anja Rabien

Received: 11 August 2010 / Accepted: 8 December 2010 / Published online: 24 December 2010  
© Springer Science+Business Media, LLC 2010

## ABSTRACT

**Purpose** The objective of this study was to investigate the effect of new 4-maleamic acid and 4-maleamide peptidyl chalcone derivatives against human prostate cancer *in vitro* and *in vivo*.

**Methods** From a series of 21 chalcones, the effects of the three best inhibitors of PC-3 and LNCaP cell viability on growth, including cell cycle changes, adhesion, migration, and cell invasion, as well as their ability to inhibit angiogenesis, clonogenic activity, and matrix metalloproteinases MMP-2 and MMP-9, were tested. The effects *in vivo* were studied in PC-3 and LNCaP xenografts.

**Results** Three of the examined chalcones reduced cell viability in both cell lines in a strong dose- and time-dependent manner. An inhibition of the cell cycle progress was observed.

These changes were accompanied with the inhibition of cell adhesion, migration, and invasion as well as with reduced neovascularization in chick embryos, tumor colony formation, and MMP-9 activity. The *in vivo* results demonstrated the strong activity of these structures as inhibitors of tumor development in nude mice compared to non-treated animals.

**Conclusion** The results suggest the multitarget efficacy of 4-maleamic acid and 4-maleamide peptidyl chalcones against human prostate cancer cells and emphasize the potential therapeutic relevance of these compounds.

**KEY WORDS** angiogenesis • chalcones • LNCaP and PC-3 xenografts • matrix metalloproteinase-9 • prostate cancer

## ABBREVIATIONS

CAM	chick chorioallantoic membrane
CI	cell index
DMSO	dimethyl sulfoxide
ECM	extracellular matrix
IC <sub>50</sub>	concentration required for 50% inhibition of the tumor cell viability
LNCaP	human prostate cancer cell line, hormone-dependent
MMP	matrix metalloproteinase
PBS	phosphate-buffered saline
PC-3	human prostate cancer cell line, hormone-independent
PCa	prostate cancer
PI	propidium iodide

J. Rodrigues • C. Abramjuk • C. Stephan • K. Jung (✉) • M. Lein • A. Rabien  
Department of Urology, University Hospital Charité  
Schumannstrasse 20/21  
10117 Berlin, Germany  
e-mail: klaus.jung@charite.de

L. Vásquez • N. Gamboa • J. Domínguez  
Laboratory of Biochemistry and Laboratory of Organic Synthesis  
School of Pharmacy, Central University of Venezuela  
Caracas, Venezuela

B. Nitzsche • M. Höpfner  
Department of Physiology, University Hospital Charité  
Berlin, Germany

R. Georgieva • H. Bäumlér  
Institute of Transfusion Medicine, University Hospital Charité  
Berlin, Germany

B. Nitzsche • C. Stephan • K. Jung • M. Lein  
Berlin Institute for Urologic Research  
Berlin, Germany

## INTRODUCTION

Prostate cancer (PCa) is the most common malignant cancer in men and the second leading cause of cancer

deaths (1). As in other tumor entities, curative therapy such as prostatectomy is limited to the organ-localized stage of PCa. In the majority of cases, PCa leads to bone metastases which become a major cause of morbidity and are present in 10–30% of all patients at the initial diagnosis (2). These patients and those with an advanced tumor after primary treatment are submitted to androgen ablation therapy. PCa is initially responsive to this hormonal therapy; however, in most cases, it becomes androgen-independent, evolving into a more aggressive androgen refractory disease. At present, the treatment modality for patients with hormonal refractory PCa is chemotherapy (3), and this treatment is currently associated with significant side effects and a reduced quality of life. Therefore, there is a need to develop novel approaches for this malignancy.

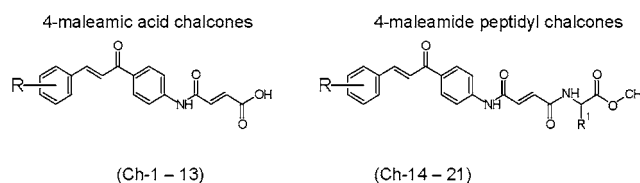
Chalcones are organic compounds that have an enone moiety between two aromatic rings. The development of these structures as potential drugs with biological properties has led to the discovery that these substances have antimalarial, anti-inflammatory, and antitumor activities (4–6). The antitumor activity of these compounds is related to the inhibition of tubulin polymerization, a decrease in the level of cyclins, thereby contributing to cell cycle arrest and an increase in the expression of Bax and Bak, but also decreases in the levels of Bcl-2 and Bcl-X(L) and subsequent activation of the mitochondrial apoptotic pathway (7,8). There are few and scarce data on the effects of chalcones on the extracellular matrix (ECM) (9,10). Since ECM proteins play an important role during adhesion, migration, invasion, and angiogenesis of cancer cells (11,12), detailed preclinical studies on the basic processes of how chalcones act as potential antineoplastic agents against PCa are necessary.

We recently synthesized a series of new 4-maleamic acid chalcones and 4-maleamide peptidyl chalcones according to a previously described procedure (5). The aim of this study was to evaluate the effect of these new compounds in *in vitro* and *in vivo* experiments as potential antitumor agents against human prostate cancer.

## MATERIALS AND METHODS

### Chalcone Compounds

Twenty-one 4-maleamic acid chalcones and 4-maleamide peptidyl chalcone compounds, synthesized according to a previous procedure (5) with structures as shown in Fig. 1, were examined in this study. The compounds were dissolved in dimethyl sulfoxide (DMSO). The final concentration of this solvent in the culture media was always lower 0.2% without a cytotoxic effect.



Compound	R
Ch-1	--
Ch-2	2,3-diMeO
Ch-3	3,4-diMeO
Ch-4	2,4-diMeO
Ch-5	2,4,5-triMeO
Ch-6	3,4,5-triMeO
Ch-7	2-MeO
Ch-8	3,4-methylenedioxi
Ch-9	4-Cl
Ch-10	2-NO <sub>2</sub>
Ch-11	3-NO <sub>2</sub>
Ch-12	4-Me <sub>2</sub> N
Ch-13	2-Cl-quinoline

Compound	R	R <sup>1</sup>
Ch-14	3,4-methylenedioxi	Phe
Ch-15	3,4-diMeO	Phe
Ch-16	3,4-dichloro	Phe
Ch-17	3,4-dichloro	Val
Ch-18	3,4-dichloro	Leu
Ch-19	--	Phe
Ch-20	4-Br	Phe
Ch-21	4-Me <sub>2</sub> N	Phe

**Fig. 1** Structure of 4-maleamic acid chalcones and 4-maleamide peptidyl chalcones.

### Cell Culture

Human prostate tumor cell lines PC-3 and LNCaP were obtained from the German Collection of Microorganisms and Cell Cultures (DSMZ, Braunschweig, Germany). Cells were grown in RPMI medium supplemented with 10% fetal bovine serum, penicillin (50 units/ml), and streptomycin (50 µg/ml), in a humidified atmosphere (95% air, 5% CO<sub>2</sub>, 37°C). Cell culture media were from Gibco-In Vitrogen, Karlsruhe, Germany and PAA Laboratories, Pasching, Austria.

### Cell Viability and Cell Growth Evaluation

A 96-well microtiter plate containing 0.1 ml of growth RPMI/well was seeded with  $5 \times 10^3$  PC-3 or  $1.2 \times 10^4$  LNCaP cells. After 24 h of culture, cells were exposed to the compounds for 72 h at concentrations ranging from 5 to 100 µg/ml. The compounds were dissolved in DMSO. The final concentration of this solvent in the culture media was always lower than 0.2%, a concentration that has neither a cytotoxic effect nor causes any interference with the colorimetric detection method. The dose-dependent effects of each compound on cell viability were assessed using the XTT test (Roche Applied Science, Mannheim,

Germany) (13). After 72 h incubation with the compounds, cells were incubated with XTT at 37°C for 4 h, and the formazan was recorded at 492 nm (Microplate reader HT II, Anthos, Salzburg, Austria). The IC<sub>50</sub> value was defined as the concentration of tested compound resulting in a 50% reduction in viability compared to vehicle-treated cells. All experiments were carried out in triplicates, with five measurements at every concentration tested. Further evaluations of the best compounds were performed using the IC<sub>50</sub> values. The time-dependent effects of the chalcones on cell growth were measured as previously described (14). Briefly, PC-3 cells ( $1 \times 10^5$ ) and LNCaP cells ( $2.4 \times 10^5$ ) were seeded in six-well plates in RPMI containing 10% fetal bovine serum and the compounds at their IC<sub>50</sub>. Trypsinized cells were counted after trypan blue staining with a hemocytometer at 24 h intervals for a period of 96 h. All experiments were carried out in triplicates.

### Cell Cycle Analysis

For cell cycle analysis, LNCaP and PC-3 cells, seeded at the previous day, were grown with their IC<sub>50</sub> of Ch-18 for 24 h and 72 h. Cells were trypsinized, washed twice in phosphate-buffered saline (PBS) and fixed overnight in 70% ethanol/PBS at -20°C. After a PBS wash, cells were incubated in the dark in a PBS solution of 300 µg/ml RNase A and 50 µg/ml propidium iodide for 30 min at room temperature. Cell cycle phases of 10,000 cells were analyzed using the flow cytometer FACSCanto II and FACSDiva software (Becton Dickinson, Franklin Lakes, NJ, USA).

### Cell Adhesion Assay

Measurements were performed using the xCELLigence Real-Time Cell Analyzer (Applied Science Roche, Mannheim, Germany). This system monitors the biological status of cells, including cell number and adhesion, by measuring electrical impedance via microelectrodes placed on the bottom of special 96-well tissue plates. The analyzer automatically measures the electrical impedance as a cell index (CI), which is transferred, analyzed, and processed by the integrated software (15). The more cells that attach onto the electrodes in the plate, the larger the impedance value, leading to a larger CI number. The results are expressed as CI and relative attachment and spreading. For the measurements, the special 96-well ACEA E-plates® were coated with fibronectin (20 µg/ml, 1 h, 37°C). The plates were washed with PBS and coated with bovine serum albumin solution in PBS (0.5%) (20 min, 37°C) after which each well was washed with PBS. Fifty µl of medium was added to record the background, and then 100 µl of PC-3 cell suspension ( $5 \times 10^5$  cells) was transferred to each well of

the ACEA E-plates® along with 50 µl of the compounds at their IC<sub>50</sub>. The adhesion and spreading of the cells were monitored every minute using this real-time cell electronic sensing system according to the manufacturer's instructions for a period of up to 4 h.

### Cell Migration and Invasion Evaluation

Cell migration was tested using the scrape wound repair assay (16). A culture of  $8 \times 10^4$  PC-3 cells was grown to confluence on 24-well plates (48 h, 37°C). A sterilized micropipette tip was used to introduce a wound across the entire cell monolayer, and the medium was removed. After washing with PBS, the chalcones were added at their respective IC<sub>50</sub> concentrations in fresh medium and incubated for 24 h in the presence of endothelial growth factor (1 pg/ml). Coverslips were mounted onto a light microscope. Images of the wounds were captured on a computer system using a digital camera immediately following wounding (0 h) and after 24 h of incubation. The wound area in each image was measured using the ImageJ program for Windows (<http://rsb.info.nih.gov/ij/>) and quantified by following the change in wound area over time compared with the original wound area. The results were expressed as the percentage of wound closure and number of migrated cells/mm<sup>2</sup>.

For the cell invasion assay, LNCaP cells ( $1 \times 10^5$  cells/ml) were pretreated with the chalcones at their IC<sub>50</sub> concentrations for 24 h. Treated cells were seeded into the upper part of the Boyden chamber membrane coated with Matrigel (Becton Dickinson Biosciences, Heidelberg, Germany) in 50 µl of serum-free media and incubated for 18 h at 37°C. The bottom of the chamber contained 500 µl of standard medium with 20% FBS. The cells that had invaded the lower surface of the chamber were reacted with calcein (4 µg/ml) in Hank's Buffered Salt Solution for 1 h at 37°C. The fluorescence of invaded cells was read at 485/530 nm (Fluoroskan Ascent, Thermo LabSystems Oy, Helsinki, Finland).

### Measurement of Clonogenic Potential

To test for anchorage-independent growth, cells were grown in 0.6% agar (17). Briefly, one milliliter of a mixture of 1.2% Noble agar (Gibco-In Vitrogen, Karlsruhe, Germany) and RPMI medium (1:1) was added into each well of a six-well plate. PC-3 and LNCaP cells ( $1 \times 10^5$ ) suspended in completed RPMI medium with 20% FBS containing 0.3% Noble agar were overlaid on the semi-solid bottom layer. The plates were kept at room temperature for 15 min and incubated for 24 h (37°C, 95% O<sub>2</sub>, 5% CO<sub>2</sub>). The following day, one milliliter of medium with the compounds at their IC<sub>50</sub> concentrations

was added to each well. After 2 weeks of incubation, the cells were stained with crystal violet (0.01%) for 18 h at 37°C. Pictures were taken under light microscopy, and the total number of colonies and the relative colony size were determined. Three sets of experiments were performed in triplicate.

### MMP Zymography

PC-3 and LNCaP cells (80% confluent in six-well plates) were washed twice with PBS and treated with the compounds at their respective IC<sub>50</sub> concentrations in 2.5 ml of serum-free medium (24 h at 37°C in a humidified atmosphere of 95% O<sub>2</sub>, 5% CO<sub>2</sub>). Twenty µl of a mixture composed of the conditioned medium and sample buffer (without mercaptoethanol, 0.75:0.25) were subjected to electrophoresis on 10% SDS-polyacrylamide gels copolymerized with 1 mg/ml of gelatin as a substrate. The gelatinolytic activity of MMP-2 and MMP-9 in the conditioned culture medium was assayed as described (18) using ImageJ Software for Windows. Pure human MMP-9 and MMP-2 protein were used as a positive control.

### Chick Chorioallantoic Membrane (CAM) Angiogenesis Assay

Fertilized chicken eggs (Lohmann Tierzucht, Cuxhaven, Germany) were kept in an incubator at 37°C in constant humidity for 3 days. After day 3, a square window was cut into the shell of each egg to assure a living embryo, and 5 ml of albumin was removed to allow detachment of the developing chorioallantoic membrane from the shell. The window was sealed with tape, and the eggs were kept in the incubator for an additional 7 days. On day 10, the tape was removed, and the CAMs were treated with the different compounds as described (19). In brief, two small rings were placed onto the CAM, and either 100 µl of vehicle (negative control) or 100 µl of the compounds at their highest IC<sub>50</sub> in the cytotoxic assay with the two cell lines were added. After 72 h, the CAMs were examined comparing alterations to control and counting the numbers of blood vessels. *In vivo* pictures were taken using a stereomicroscope equipped with a Kappa digital camera system.

### PC-3 and LNCaP Xenografts

Male athymic nude BALB/c (nu/nu) mice (Taconic Europe, Ejby, Denmark, 5–7 weeks old, different batches for the two cell lines PC-3 and LNCaP) were maintained in accordance with the Institutional Animal Care and Use Committee guidelines, Germany. After one week of settling in for the mice, a suspension of tumor cells (PC-3 and LNCaP, respectively) in complete

culture medium was mixed with BD Matrigel Matrix High Concentration (Becton Dickinson) in a 1:1 ratio. A suspension of 1 × 10<sup>6</sup> cells (0.1 ml) was injected subcutaneously into the left flank of each mouse. Tumor volume was calculated every 24 h using a caliper and following the formula  $V = \frac{\pi}{6} * 1.69 * (length * width)^{3/2}$  (20).

Mice were randomized into groups of either 7 (LNCaP experiment) or 10 animals (PC-3 experiment), and treatment was started when a tumor was palpable in each animal. In the test groups, compounds were dissolved in DMSO and suspended in saline solution-Tween 20 (2%) to a final concentration of 4 mg/kg to be injected intraperitoneally. For PC-3 xenografts, tumors were palpable one week following the cell inoculation and were then treated every 24 h for 21 consecutive days, while for LNCaP xenografts, tumors were well developed 25 days following the cell inoculation and were then treated every 24 h for 5 consecutive days. Control mice were injected with vehicle. At the end of the experiment, animals were euthanized by cervical dislocation.

### Statistical Analysis

Statistical analysis was performed by Student's t-tests and one-way ANOVA using the software SPSS version 18.0 (SPSS, Chicago, IL, USA). *P*-values < 0.05 (two-tailed) were regarded as significant. IC<sub>50</sub> values were calculated by nonlinear regression of experimental data using the equation  $Y = \frac{Bottom + (Top - Bottom)}{1 + 10^{(log(IC_{50} - X) * Hilllope)}}$  of the program GraphPad Prism (GraphPad Software, San Diego, CA, USA), where X is logarithm of concentration and Y is the response.

## RESULTS

### Effects of Chalcones on the Viability and Cell Growth

A series of new acid chalcones and peptidyl chalcones were tested for their ability to inhibit the viability of the human PCa cell lines PC-3 and LNCaP (Fig. 1). The results are summarized in Table I. From a total of 21 compounds, six inhibited PC-3 cell viability (IC<sub>50</sub> < 100 µg/ml), and the three best compounds (Ch-10, Ch-18 and Ch-20) also had a significant effect on LNCaP tumor cells (Table I). The effect of Ch-10, Ch-18, and Ch-20 on cell viability was dose-dependent in both of the cell lines tested, showing reduced viability from 5 µg/ml onwards (Fig. 2a, b). The activity of these compounds at their IC<sub>50</sub> concentrations was also time-dependent (Fig. 3a, b). The different inhibition effects of the chalcones observed in the dose-response and time-course studies were apparently caused by the use of different methods. The dose-response curves

**Table 1** Cytotoxic Effect of 4-Maleamic Acid Chalcones and 4-Maleamide Peptidyl Chalcones on Human Prostate Tumor Cells Indicated as Half Inhibitory Concentration

Compounds <sup>a</sup>	IC <sub>50</sub> (μg/ml) <sup>b</sup>	
	PC-3 cells	LNCaP cells
Ch-1	> 100	> 100
Ch-2	> 100	> 100
Ch-3	> 100	> 100
Ch-4	> 100	> 100
Ch-5	> 100	> 100
Ch-6	> 100	> 100
Ch-7	98.8 ± 0.01	> 100
Ch-8	80.5 ± 5.0	> 100
Ch-9	63.3 ± 5.2	> 100
Ch-10	38.9 ± 3.5	44.1 ± 2.8
Ch-11	> 100	> 100
Ch-12	> 100	> 100
Ch-13	> 100	> 100
Ch-14	> 100	> 100
Ch-15	> 100	> 100
Ch-16	> 100	> 100
Ch-17	> 100	> 100
Ch-18	29.5 ± 1.5	21.4 ± 2.0
Ch-19	> 100	> 100
Ch-20	56.9 ± 0.26	45.9 ± 1.9
Ch-21	> 100	> 100

<sup>a</sup> Detailed structures of the chalcones are given in Fig. 1.

<sup>b</sup> IC<sub>50</sub> values were calculated by nonlinear regression using the equation  $Y = \frac{\text{Bottom} + (\text{Top} - \text{Bottom})}{1 + 10^{(\log \text{IC}_{50} - X) \cdot \text{Hilllope}}}$ , where X is logarithm of concentration and Y is the response. Results are expressed as mean ± SEM of three different experiments.

were established with the XTT assay, while the time-course experiments were done in a low density environment, and the cells were counted after trypan blue staining with a hemocytometer.

Results of the cell cycle analysis of IC<sub>50</sub> Ch-18-treated cells are shown as exemplary histograms for LNCaP cells (Fig. 4a, b) and PC-3 cells (Fig. 4c, d), respectively, and as summarized distribution pattern (Fig. 4e, f). Comparison of LNCaP control cells (Fig. 4a) and LNCaP Ch-18 cells (Fig. 4b) showed a trend to increased sub-G1 and decreased G0/G1 phases (Fig. 4e;  $p=0.086$  and  $p=0.091$ , respectively). The increase in sub-G1 was more pronounced in PC-3 cells (Fig. 4f; 17.1%), comparing PC-3 control cells (Fig. 4c) with PC-3 Ch-18 cells (Fig. 4d), and accompanied by a considerable decrease of G0/G1 phases (Fig. 4f; 31.8%). After exposure to Ch-18, there was a significant accumulation of PC-3 cells in the S and G2/M phases, whereas LNCaP cells did not show it (Fig. 4e, f).

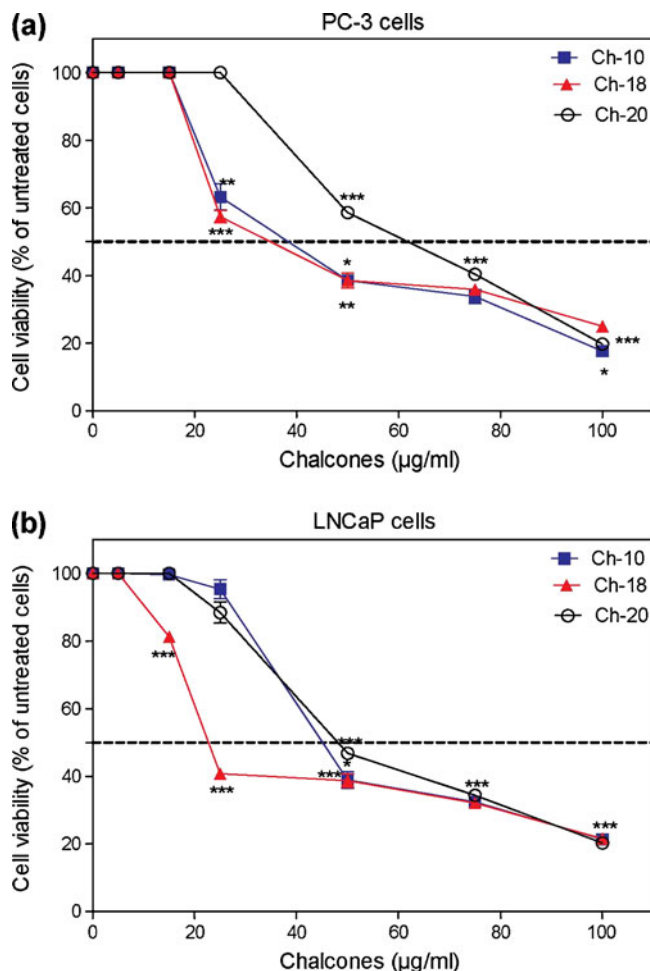


**Fig. 2** Dose-response curves for PC-3 (a) and LNCaP cells (b) treated with 4-maleamic acid and 4-maleamide peptidyl chalcones. After 72 h incubation with the compounds, cells were incubated with XTT at 37°C for 4 h and the formazan was recorded at 492 nm. Results are expressed as means ± SEM,  $n=3$ . Data were analyzed by Student's *t*-test. Significances: \* $p < 0.05$ , \*\* $p < 0.01$ , and \*\*\* $p < 0.001$  compared to the same treatment at the previous concentration.

### Effects of Chalcones on the Adhesion, Spreading, Migration, and Invasion

Chalcones inhibited cell attachment and spreading at their cytotoxic IC<sub>50</sub> concentrations (Fig. 5a, b).

To examine the effect of the chalcones on the migration properties of the tumor cells, the wound-healing scratch assay was used (16). Control chalcone-free cultures of PC-3 cells generally displayed wound recovery within 24 h and migration of cells to the wound (Fig. 6a). Chalcones at their IC<sub>50</sub> reduced the ability to close the scrape wound and decreased the number of migrating cells (Fig. 6b, c; not tested on LNCaP cells). The results of the cell invasion assay revealed that chalcones at IC<sub>50</sub> also decreased invasion significantly (Fig. 7; not tested on PC-3 cells). This effect was remarkable, since the inhibition was already

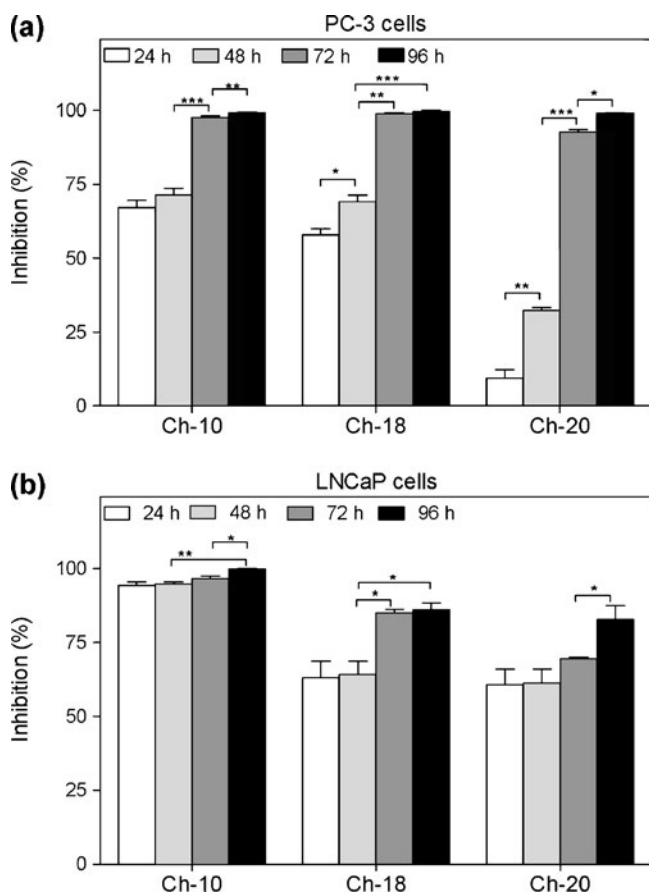


**Fig. 3** Time-response effects of 4-maleamic acid and 4-maleamide peptidyl chalcones at their  $IC_{50}$  concentrations on PC-3 (a) and LNCaP (b) cell growth. PC-3 cells ( $1 \times 10^5$ ) and LNCaP cells ( $2.4 \times 10^5$ ) were seeded in six-well plates in RPMI containing 10% FBS and the compounds at their  $IC_{50}$ . Cells were collected from culture dishes after trypsin-EDTA treatment for 7 min at  $37^\circ\text{C}$ , and the number of viable cells per well was counted after trypan blue staining with a hemocytometer at 24 h intervals for a period of 96 h. Results are expressed as means  $\pm$  SEM. Data were analyzed by Student's *t*-test. Significances are as in Fig. 2.

detectable in LNCaP cells, which have a lower invasive capacity than PC-3 cells.

### Effects of Chalcones on the MMP-9 Activity

As shown in Fig. 8, the chalcone compounds decreased MMP-9 activity in PC-3 and LNCaP cells at  $IC_{50}$ , whereas we did not detect any MMP-2 activity in either cell lines, as also previously reported by Kumar *et al.* (21) in the same tumor cell lines.

### Effects of Chalcones on the Neoangiogenesis

In the control CAM, a regular vascular network with a continuously perfused capillary plexus supplying branched vessels was shown (Fig. 9a). The chalcone compounds at  $IC_{50}$  induced a degeneration of the vascular network.

Unperfused areas and changes in branching of the small supplying vessels were characteristic of these alterations, suggesting the potential antiangiogenic properties of these structures (Fig. 9b, c, d). In addition, the number of the newly formed blood vessels was significantly reduced (Fig. 9e).

### Effects of Chalcones on the Colony Formation

Anchorage-independent growth is considered an *in vitro* test, which correlates with tumorigenesis in nude mice (22). We examined the ability of PC-3 and LNCaP cells to grow in a semisoft agar medium. All the controls showed significant growth in soft agar, forming colonies on day 14 (Fig. 10). In cells treated with the chalcones at their  $IC_{50}$ , colonies were either reduced in size or number or even completely absent (Fig. 10, Table II).

### Effects of Chalcones on the Tumor Growth of PC-3 and LNCaP Xenografts

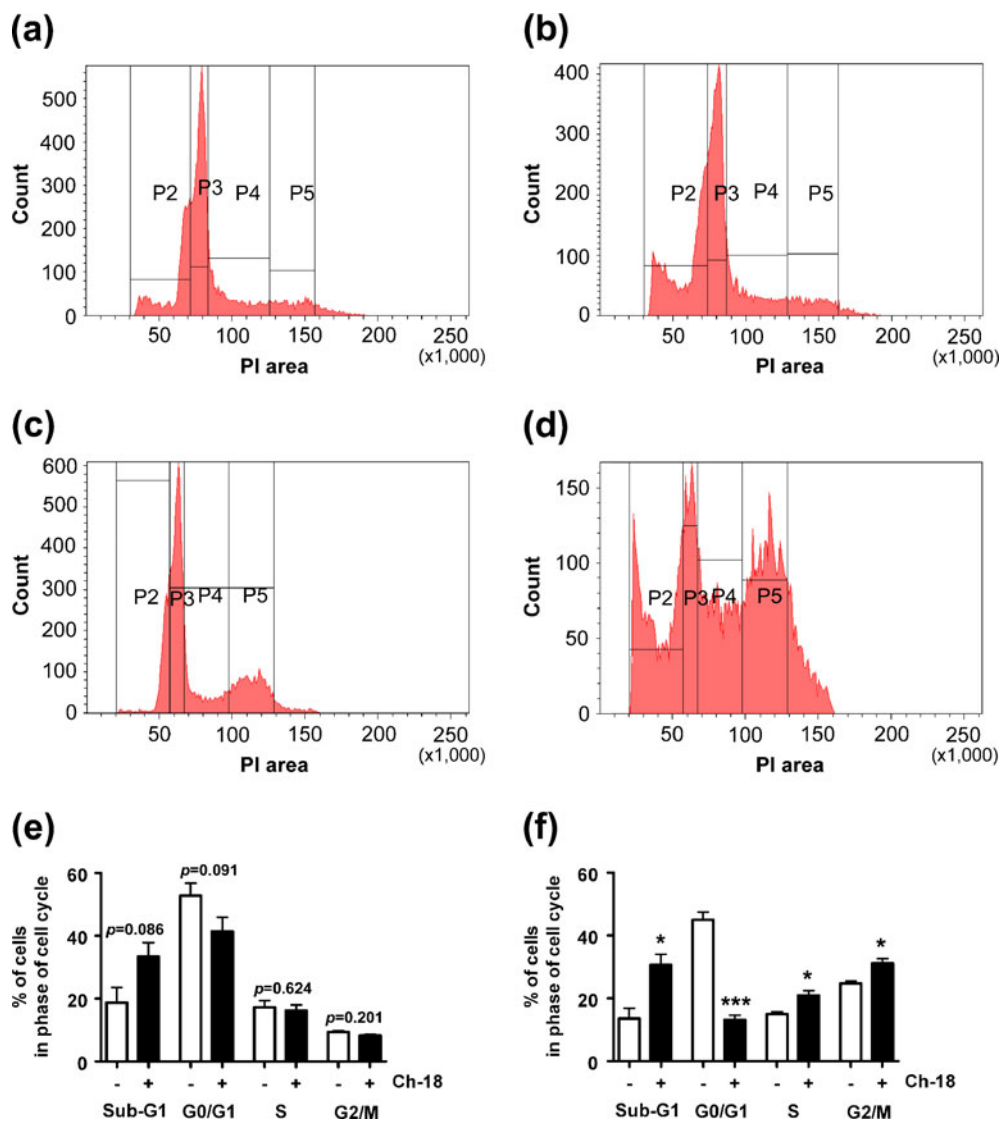
Due to the promising results *in vitro*, we tested the ability of these chalcones (4 mg/kg body weight; intraperitoneal) to inhibit tumor growth *in vivo* in PC-3 and LNCaP xenografts. Mice bearing PC-3 xenografts and treated with the chalcones showed distinctly lower tumor volumes compared to non-treated mice (vehicle), from the second day of therapy until day 21 of treatment (Fig. 11a). It is remarkable that the initial tumor volume even decreased within the first ten days of treatment. In order to verify the effects of the chalcones on a different *in vivo* tumor model, we also tested their ability to inhibit tumor development in LNCaP xenografts. The results showed that the compounds inhibited tumor growth from the beginning of therapy until the fifth day of treatment, at which point the experiment was terminated (Fig. 11b).

The applications of the chalcones were well tolerated, as indicated by the behaviour of the animals and by the body weight observed both in the controls and treatment groups. In the PC-3 xenograft experiment, the mean ( $\pm$ SD) body weight of the control group was 29.1 ( $\pm$ 1.73) g *vs.* 27.7 ( $\pm$ 2.57) g of all treated animals at the beginning of the treatment in comparison with 30.3 ( $\pm$ 1.73) g and 29.1 ( $\pm$ 2.74) g at the end of the treatment. In the LNCaP experiment, the corresponding data were 22.7 ( $\pm$ 1.60) g *vs.* 23.1 ( $\pm$ 1.56) g at the beginning and 22.9 ( $\pm$ 1.95) g *vs.* 23.5 ( $\pm$ 1.78) g at the end of the experiment.

## DISCUSSION

As briefly mentioned in the introduction, chalcones have been reported as possible antitumor agents, showing effects against neuroblastoma, breast, bladder, colon, and leukemia cancer cells (6,7,23–25). Their mechanisms of action

**Fig. 4** Cell cycle analysis of LNCaP and PC-3 cells treated with Ch-18. After incubation with the  $IC_{50}$  of Ch-18 (29.5  $\mu\text{g/ml}$  for PC-3 and 21.4  $\mu\text{g/ml}$  for LNCaP cells), fixed propidium iodide stained cells were analyzed using flow cytometry. Representative histograms are given: **a** LNCaP cells, controls; **b** LNCaP cells, treated; **c** PC-3 cells, controls; **d** PC-3 cells, treated. Symbols P2, P3, P4, and P5 represent sub-G1, G0/G1, S, and G2/M phases, respectively. Data for cell cycle phases for LNCaP cells (**e**) and PC-3 cells (**f**) are means  $\pm$  SEM,  $n=4$ . Significances (paired Student's *t*-test) as in Fig. 2 for PC-3 cells (**f**); *p*-values for LNCaP (**e**) are given to demonstrate the trend.



involve the tubulin assembly inhibition, antiangiogenic effects, reactive oxygen species generation, and apoptosis induction through the release of cytochrome *c* and activation of caspase-9 and the inhibition of the nuclear factor kappa B survival system (7,8,26,27). More recent studies have shown the effect of different chalcones on PCa, demonstrating substantial *in vitro* anti-proliferative activities in LNCaP and PC-3 human prostate cancer cell lines as antagonists of androgen receptors (28). However, there is no information on compounds that share this chemical activity against prostate cancer *in vivo*.

In this study, we demonstrated the *in vitro* and *in vivo* antitumor activity of new 4-maleamic acid chalcones and 4-maleamide peptidyl chalcones against human prostate cancer. Twenty-one compounds were tested, and three of them (compounds Ch-10, Ch-18 and Ch-20) were active against both androgen-independent (PC-3) and androgen-sensitive (LNCaP) human PCa cells. Special attention was

paid to compound Ch-18, a 4-maleamide peptidyl chalcone analog with a leucine amino acid as a substituent group, which was the most cytotoxic compound in both tumor cell lines ( $IC_{50}$  of 29.5  $\mu\text{g/ml}$  for PC-3 cells and 21.4  $\mu\text{g/ml}$  for LNCaP cells). These three active compounds demonstrated the most potent antitumor effects, and we suggest that the nitro group, the dichloride and the bromide atoms located in the aromatic ring of the  $\alpha,\beta$ -unsaturated ketone system (Fig. 1) play an important role in mediating the activity as antitumorals. They may cause stronger chemical interaction with the biological substrate due to their lipophilic, electronegative and electron withdrawing inductive effects. On the other hand, our results showed that the incorporation of an amino acid to form the peptidyl compounds increased the activity. This clearly indicates that lipophilic together with electrostatic interactions are responsible for improving their effects. We could notice that the replacement of the withdrawing groups by the hydrophilic and electron-donating groups such as

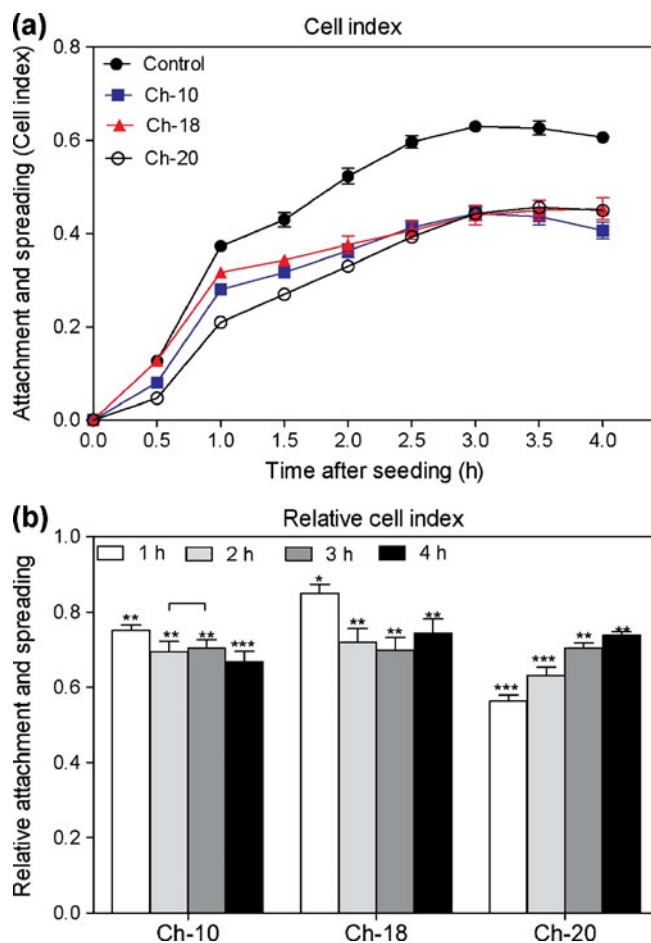


**Fig. 5** Effect of chalcone compounds on cell adhesion. Measurements were performed with xCELLigence Real-Time Cell Analyzer (Roche). **(a)** PC3 cells were incubated with the chalcones at their  $IC_{50}$  (Ch-10 = 38.9  $\mu\text{g}/\text{ml}$ , Ch-18 = 29.5  $\mu\text{g}/\text{ml}$ , and Ch-20 = 56.9  $\mu\text{g}/\text{ml}$ ). The cells were applied onto the fibronectin-coated sensors, and their attachment and spreading were quantified by real-time cell electronic sensing as cell index values (CI). **(b)** The extent of attachment and spreading over the time post-seeding was also quantified by plotting the relative cell index for vehicle-control (medium-DMSO, 0.2%) and chalcones-treated cells (means  $\pm$  SEM,  $n=3$ ). Data were analyzed by Student's *t*-test. Significances: \* $p < 0.05$ , \*\* $p < 0.01$ , and \*\*\* $p < 0.001$  compared to vehicle (relative cell index of 1.0).

methoxy and 3,4-methylenedioxy in the aromatic ring decreased the activity. We also demonstrated that compound Ch-17, which has both lipophilic attachments in the aromatic ring, including the incorporation of a terminal amino acid moiety, did not show antitumor actions. In this context, the biological substrate could prefer a more electronic volume to interact, which is the case of leucine instead of valine and a more hydrophobic amino acid like leucine instead of phenylalanine in the case of compound Ch-16, suggesting that some electronic and lipophilic effects would take place. These findings confirm that the antitumor activity of the compounds correlates to the lipophilic nature together with the electronic parameters of the amino acid moiety, the halogens and nitro groups of the molecules.

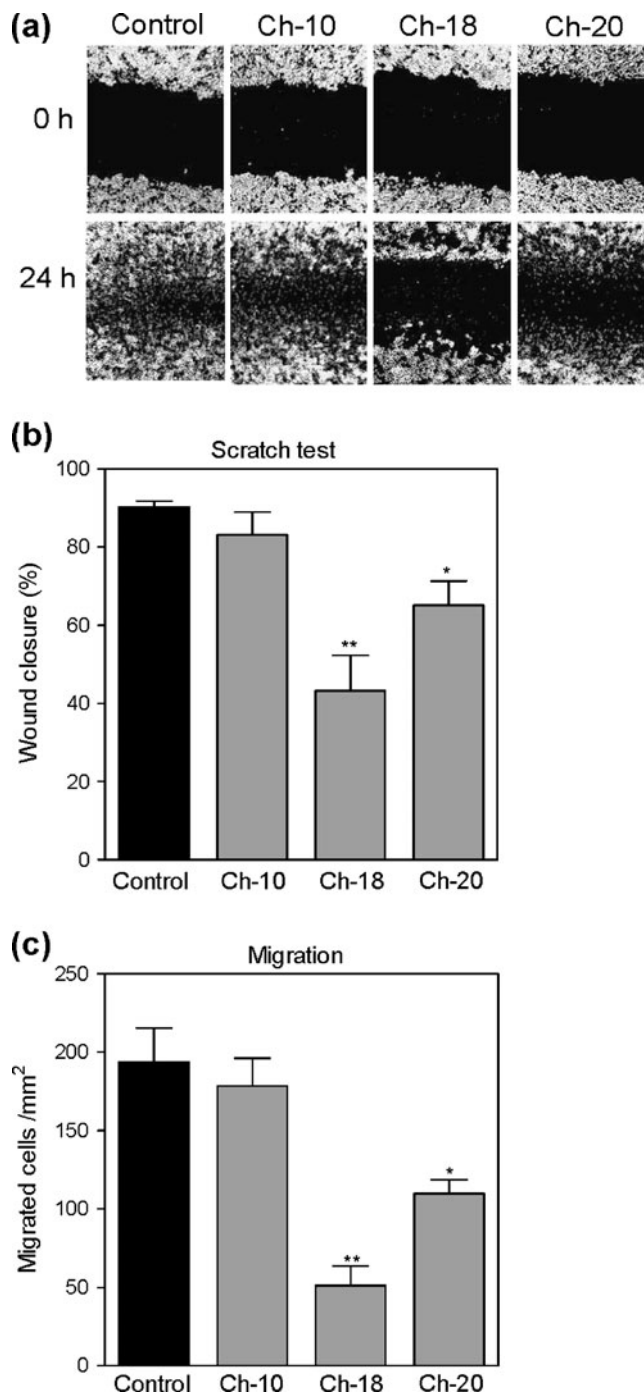


**Fig. 6** Effect of chalcone compounds on wound closure in a single scrape wound model on PC-3 cells. **(a)** Representative contrast images of PC-3 cells were captured at the time of wounding and 24 h following the wound to illustrate recovery from scrape wound. **(b)** The percentage of wound area closed at 24 h post-treatment is plotted for cell monolayers with the chalcones at their  $IC_{50}$  (Ch-10 = 38.9  $\mu\text{g}/\text{ml}$ , Ch-18 = 29.5  $\mu\text{g}/\text{ml}$ , and Ch-20 = 56.9  $\mu\text{g}/\text{ml}$ ) or without. **(c)** The number of migrated cells was also plotted after 24 hours post-treatment. Data in **(b)** and **(c)** are means  $\pm$  SEM,  $n=3$ . Data were analyzed by Student's *t*-test. Significances: \* $p < 0.05$  and \*\* $p < 0.01$  compared to controls.



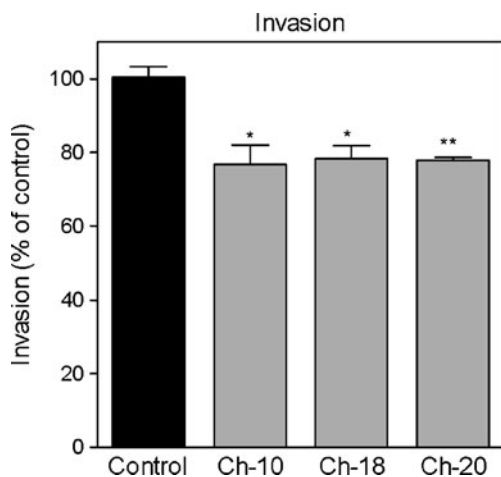


**Fig. 7** Effect of chalcones on the invasion of LNCaP cells. Cells treated with the chalcones (Ch-10 = 44.1  $\mu\text{g/ml}$ , Ch-18 = 21.4  $\mu\text{g/ml}$ , and Ch-20 = 45.9  $\mu\text{g/ml}$ ) or the vehicle were seeded onto a Matrigel-coated 0.8  $\mu\text{m}$  porous membrane for 18 h, and the inhibition of invasion relative to the control vehicle treated cells was determined (means  $\pm$  SEM,  $n=3$ ). Data were analyzed by Student's *t*-test. Significances are as in Fig. 2.

The inhibitory activity of each of these three compounds at their  $\text{IC}_{50}$  was evident from the first day of incubation. After 72 h of exposure of each of the three substances to both cell lines, there was almost 100% inhibition of cell

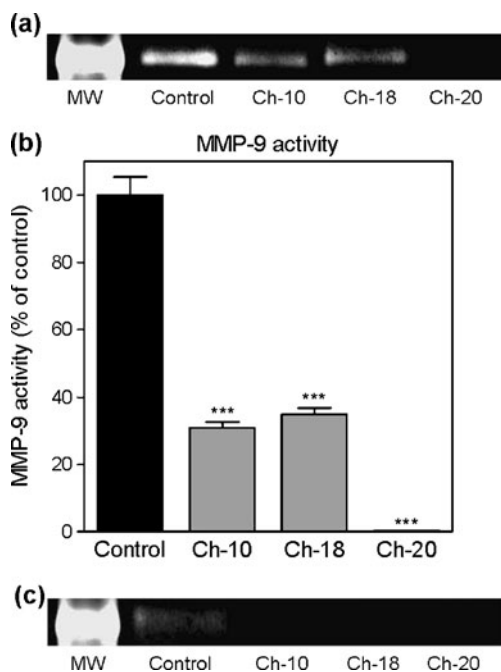


**Fig. 8** Activity of MMP-9 metalloproteinase by gelatin zymography in PC-3 (a, b) and in LNCaP cells (c) when exposed to chalcones for 24 h (Ch-10 = 38.9  $\mu\text{g/ml}$ , Ch-18 = 29.5  $\mu\text{g/ml}$ , and Ch-20 = 56.9  $\mu\text{g/ml}$  for PC-3 cells and Ch-10 = 44.1  $\mu\text{g/ml}$ , Ch-18 = 21.4  $\mu\text{g/ml}$ , and Ch-20 = 45.9  $\mu\text{g/ml}$  for LNCaP cells). Conditioned media prepared from subconfluent cultures were collected and processed for zones of gel degradation activity. Only the results in PC-3 cells (b) were quantified in relation to controls (means  $\pm$  SEM,  $n=3$ ). Data were analyzed by Student's *t*-test. \*\*\* $p < 0.001$  compared to control vehicle.

growth. The inhibition was dose- and time-dependent, partly more efficient than described by isoliquiritigenin, another chalcone (9).

Cell cycle analyses of  $\text{IC}_{50}$  Ch-18-treated cells showed characteristic changes in PC-3 cells and similar trends in LNCaP cells. We observed an increased proportion of the treated cells in the G2/M and sub-G1 phases accompanied by a decreased proportion of cells in the G0/G1 phase. Similar data were recently shown in Jurkat cells with other chalcones that were related to the cell cycle arrest at the G2/M phase (29). A G2/M accumulation of cells induced by other chalcones was described in different tumor cells (7,9,30–32). This effect was time- and dose-dependent as well as dependent on the chalcone used. In addition, as shown in our example of LNCaP and PC-3 cells and in other cells, the chalcone-induced effect of cell arrest is also cell-dependent (29). Thus, all these results and data evidence that at least one of the anti-cancer mechanisms of the chalcones is their cell cycle arrest-inducing effect. However, the exact molecular mechanism remains to be elucidated.

Metastasis is the main cause of morbidity and mortality in patients with cancer. The basis of this event is explained by consecutive processes that include the adhesion of tumor cells to the basement membrane, local proteolysis that leads to the migration of tumor cells through the stroma and the invasion of cells into the capillary wall, thus entering the blood and leading to tumor cell spread into other organs (33). During the process of metastasis, the invasion of cancer cells is the most important and characteristic step. An agent that inhibits the growth and invasion of these cells would be a hopeful candidate for suppressing cancer development. The adhesion and migration of cancer cells are also important steps leading to invasion. Our results indicate that the chalcones tested act as inhibitors of cell attachment and migration.

MMPs are also involved in cell migration by removing sites of adhesion, exposing new binding sites, cleaving cell-cell or cell-matrix receptors, and releasing chemoattractants from the ECM (34). In this context, these proteases are involved in tumor development, establishing a microenvironment that is appropriate for metastatic growth, and angiogenesis for sustained growth. Thus, MMPs contribute to the carcinogenic process at multiple stages, including invasion, migration and angiogenesis, thus leading to metastasis, and therefore represent an important target (11,35,36). Our results showed that a possible mechanism by which our chalcone compounds may inhibit tumor cell attachment, migration, and invasion is the down-regulation of the MMPs, since the compounds blocked the activity of MMP-9. After 24 h of treatment, the activity of MMP-9 was reduced by more than 50% compared to the controls. Particular attention was paid to compound CH-20, which inhibited MMP-9 almost completely in PC-3 cells. A recent study that experimented with a hydrox-

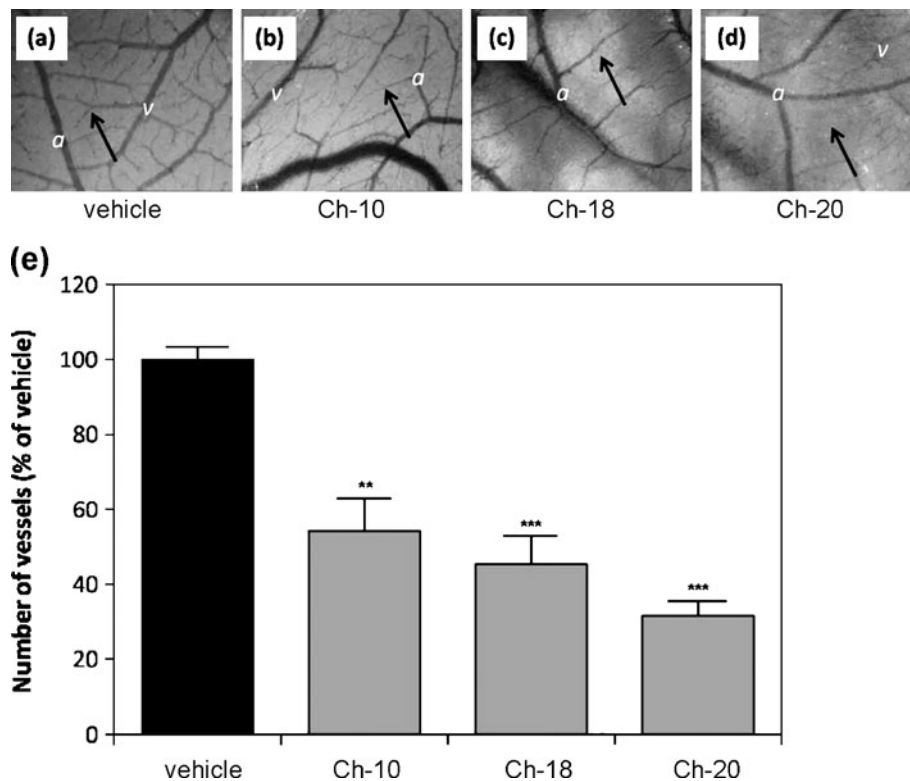


**Fig. 9** Blood vessel degeneration and reduced neovascularization by treatment of developing chicken chorioallantoic membrane (CAM) with chalcone compounds. Representative pictures show CAMs on day 13 of development, treated with (a) vehicle, (b) Ch-10 (44.1  $\mu\text{g/ml}$ ), (c) Ch-18 (29.5  $\mu\text{g/ml}$ ) or (d) Ch-20 (56.9  $\mu\text{g/ml}$ ) for 72 h ( $a$  = artery and  $v$  = vein). In the control CAM (a), the vascular network consists of a continuously perfused capillary plexus and supplying vessels. The vessels are arranged symmetrically and have characteristic branches (arrow). Chalcones (b, c, d) induced a degeneration of the vascular network shown as unperfused areas and changes in branching of the small supplying vessels. (e) Quantification of newly formed blood vessels in 16 CAMs (4 eggs each compound). Numbers of blood vessels were counted in four sections of each CAM. Changes are shown as percentage in relation to control (means  $\pm$  SEM,  $n=4$ ). Data were analyzed by Student's  $t$ -test. Significances are as in Fig. 2.

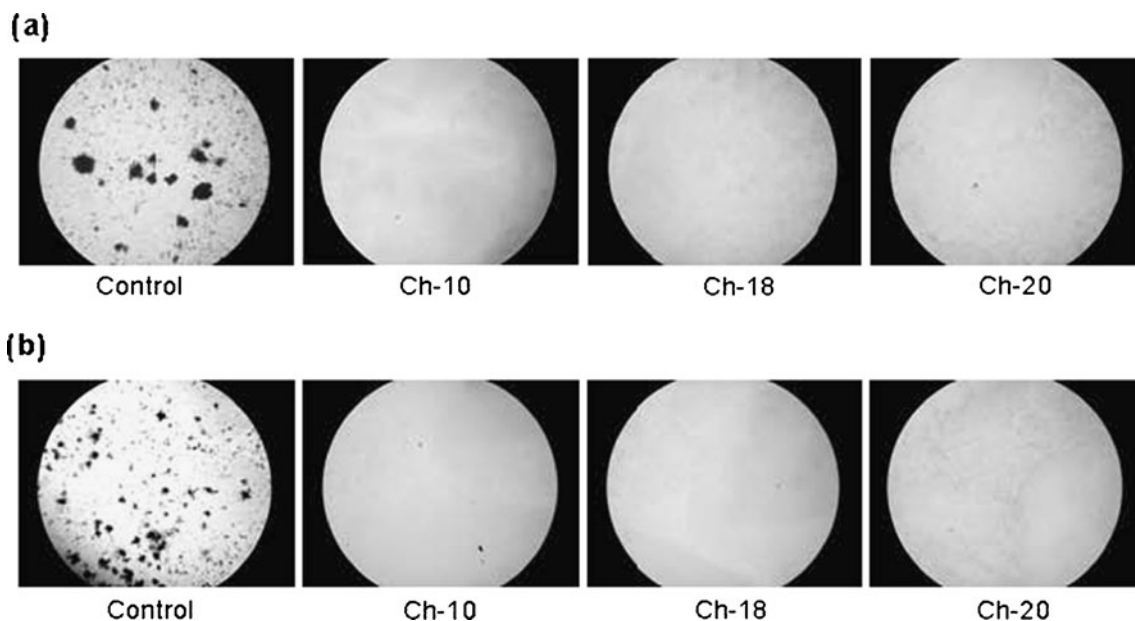


**Fig. 10** Effect of the chalcone compounds on the formation of colonies in soft agar. PC-3 (a) and LNCaP cells (b) were plated over a semi-solid layer of soft agar, treated with the chalcones (Ch-10=38.9  $\mu\text{g/ml}$ , Ch-18=29.5  $\mu\text{g/ml}$ , and Ch-20=56.9  $\mu\text{g/ml}$  for PC-3 cells and Ch-10=44.1  $\mu\text{g/ml}$ , Ch-18=21.4  $\mu\text{g/ml}$ , and Ch-20=45.9  $\mu\text{g/ml}$  for LNCaP cells), and incubated for 14 days. The results represent standard images of three different experiments.

**Table II** Inhibition of Clonogenic Growth Potential of Prostate Cancer Cells by Chalcones

Parameter	Controls	Chalcones		
		Ch-10	Ch-18	Ch-20
Colony formation, %				
PC-3 cells	100 ± 17.6	1.22 ± 0.09***	0	0
LNCaP cells	100 ± 18.3	0.03 ± 0.02***	0	0
Relative colony size				
PC-3 cells	1 ± 0.30	0.01 ± 0.01***	0	0
LNCaP cells	1 ± 0.05	0.025 ± 0.02**	0	0

Colony growth relative to non-treated PC-3 and LNCaP cells were quantified, and the results given are means ± SEM of three independent experiments. Significances: \*\* $p < 0.01$  and \*\*\* $p < 0.001$  compared to control vehicle

ychalcone also showed an inhibitory effect on the MMP-9 expression in the PCa cell line DU-145 (10).

Inhibitors of MMPs, such as the synthetic MMP inhibitor batimastat, blocked vascular invasion and tubule formation *in vitro*, two of the steps that are necessary for successful angiogenesis (37). Our results showed that our chalcones also inhibited angiogenesis according to the chick embryo CAM model, suggesting the potential antiangiogenic effect of these structures, as previously shown with the 2-hydroxy-4-methoxy chalcone via the blockade of the vascular endothelial growth factor receptor signal pathway (26,38). The effect of the chalcones on MMP-9 could also be responsible for this inhibition of angiogenesis (39).

Neoangiogenesis can be initiated by the release of pro-angiogenic factors (*e.g.*, VEGF, bFGF, and tumor necrosis factor- $\alpha$ ) which bind to their respective cell-surface receptors on endothelial cells, leading to their activation, which involves the induction of cell proliferation, increased expression of cell adhesion molecules, secretion of MMPs, and increased migration and invasion (40,41). It is possible that our chalcones also inhibited the production of these pro-angiogenic factors, especially VEGF, leading to the effects that are reported in this study. Further studies should be performed to test this hypothesis, along with other mechanisms of action, since another chalcone compound (2'-hydroxy-4'-methoxychalcone) was reported to be an antiangiogenic compound due to its anti-proliferative activity following inhibition of the induction of COX-2 enzyme *in vitro* and *in vivo* (26).

Tumor cells are able to grow in soft agar, which distinguishes them from normal non-tumorigenic cells (22). This feature of phenotypic transformation has been correlated with the *in vivo* development of murine tumor cells and metastasis, since low-metastatic-potential cells did not form visible colonies in Noble agar medium, indicating the ability of these cells to avoid growth-dependent

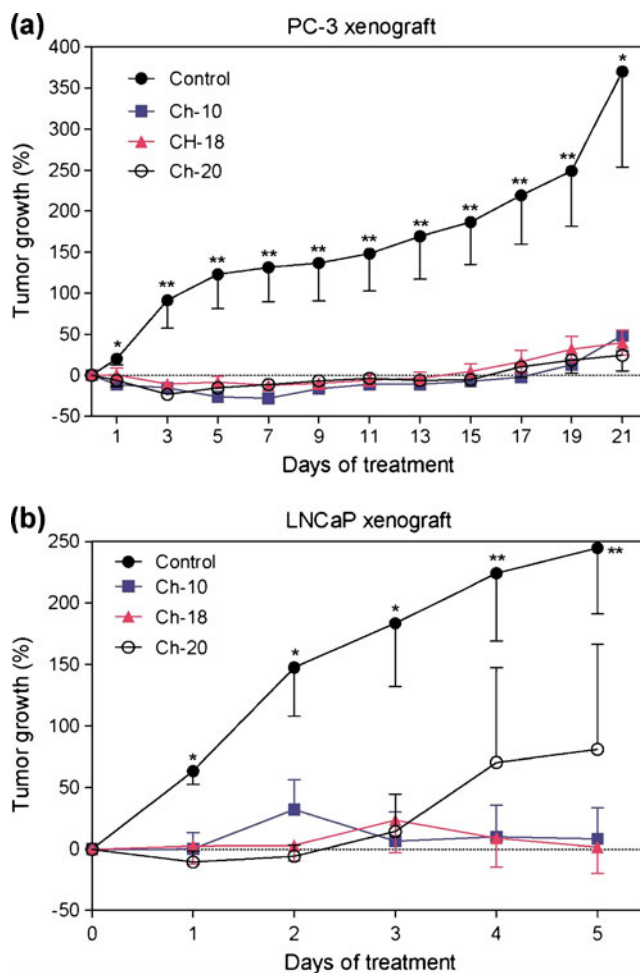


**Fig. 11** *In vivo* antitumor activity of the chalcones in PC-3 and LNCaP xenografts. Seven and 25 days after the injection of PC-3 (a) and LNCaP (b) cells, respectively, the animals were treated every day (4 mg/kg body weight, intraperitoneal injection). The results are expressed as the mean ± SEM of 10 animals in each group of the PC-3 experiment and seven in each group of the LNCaP experiment given as percentage of the initial tumor volume. Data were analyzed by Student's *t*-test. Significant differences of at least \* $p < 0.05$  and \*\*\* $p < 0.01$  between controls and treated animals except for Ch-20 treated animals at day 4 ( $p = 0.077$ ) and day 5 ( $p = 0.082$ ).

regulatory mechanisms (42). Our results showed that PC-3 or LNCaP cells developed into relatively large colonies, whereas those cultured with the chalcone compounds at their  $IC_{50}$  resulted in fewer and smaller-sized colonies for Ch-10 or the complete abolishment of colonies (Ch-18 and Ch-20), indicating the loss of the transformed phenotype.

These compounds were also tested in tumor murine models, since there have not been *in vivo* studies regarding the effects of chalcones in prostate cancer until now. Mice with PC-3 xenograft implants treated with the chalcones showed significant decreases in their tumor volumes compared to vehicle-treated mice from the second day of therapy until day 21 of treatment, indicating substantial

activity *in vivo*. The chalcones were also evaluated in a tumor murine model with different growth kinetics. Thus, treatments were administered to mice bearing LNCaP xenografts, which contained larger tumors. Treated mice showed a reduction in tumor growth compared with controls from the very first day until the fifth day of therapy, suggesting that the chalcones could also be an option against a more progressive cancer. Moreover, no toxic effects in animals were observed at the dose tested during the entire assays. It is important to note that the use of only 4 mg/kg gave promising results; the effect could probably be improved by increasing the dose. However, the strict regulations for animal experiments did not allow a dose-finding trial in animals in these preliminary experiments.

Overall, our results demonstrated that the *in vitro* antitumor activity of the derivatives is mirrored by their properties *in vivo*, and several mechanisms of the anti-cancer effect have to be considered. We noted the potential anticancer actions of these new chalcones either in their acid form or with a peptide substituent. However, the presence of a 2-NO<sub>2</sub> substitution in the phenyl group of the acid chalcones and a halogen atom in the phenyl group of the peptidyl chalcones seems to improve activity, along with the incorporation of a leucine. Our data show that several mechanisms of the anti-cancer effect of chalcones have to be considered. Since the chalcones affect the different basic processes, such as adhesion, proliferation, migration, invasion, and clonogenic activity of prostate cancer cells, as well as the angiogenesis, a multitarget action can be assumed. Drugs that simultaneously attack different molecules offer advantages in comparison to drugs selective for a single target (43). These promising *in vitro* results and the inhibition of tumor development *in vivo* could constitute the basis for future research to explain the exact molecular mechanism for using these chalcones as potential anti-prostate cancer agents.

## ACKNOWLEDGMENTS

This study was partly supported by grants from the Foundation for Urological Research to CA, JR, and ML (Grant no. GRUB\_3), Berlin, Germany and the German Academic Exchange Service (DAAD) to JR (Grant no. Referat 414, \_A/07/98623). We thank Sabine Becker for her valuable technical assistance and two unknown reviewers for their helpful suggestions to improve the manuscript.

## REFERENCES

- Jemal A, Siegel R, Ward E, Hao Y, Xu J, Thun MJ. Cancer statistics, 2009. *CA Cancer J Clin*. 2009;59:225–49.
- Logothetis CJ, Lin SH. Osteoblasts in prostate cancer metastasis to bone. *Nat Rev Cancer*. 2005;5:21–8.
- Dreicer R. Current status of cytotoxic chemotherapy in patients with metastatic prostate cancer. *Urol Oncol*. 2008;26:426–9.
- Alcaraz MJ, Vicente AM, Araico A, Dominguez JN, Terencio MC, Ferrandiz ML. Role of nuclear factor-kappaB and heme oxygenase-1 in the mechanism of action of an anti-inflammatory chalcone derivative in RAW 264.7 cells. *Br J Pharmacol*. 2004;142:1191–9.
- Dominguez JN, Leon C, Rodrigues J, de Gamboa DN, Gut J, Rosenthal PJ. Synthesis and evaluation of new antimalarial phenylurenyl chalcone derivatives. *J Med Chem*. 2005;48:3654–8.
- Liu X, Go ML. Antiproliferative activity of chalcones with basic functionalities. *Bioorg Med Chem*. 2007;15:7021–34.
- Shen KH, Chang JK, Hsu YL, Kuo PL. Chalcone arrests cell cycle progression and induces apoptosis through induction of mitochondrial pathway and inhibition of nuclear factor kappa B signalling in human bladder cancer cells. *Basic Clin Pharmacol Toxicol*. 2007;101:254–61.
- Romagnoli R, Baraldi PG, Carrion MD, Cara CL, Cruz-Lopez O, Preti D, et al. Design, synthesis, and biological evaluation of thiophene analogues of chalcones. *Bioorg Med Chem*. 2008;16:5367–76.
- Kanazawa M, Satomi Y, Mizutani Y, Ukimura O, Kawauchi A, Sakai T, et al. Isoliquiritigenin inhibits the growth of prostate cancer. *Eur Urol*. 2003;43:580–6.
- Kwon GT, Cho HJ, Chung WY, Park KK, Moon A, Park JH. Isoliquiritigenin inhibits migration and invasion of prostate cancer cells: possible mediation by decreased JNK/AP-1 signaling. *J Nutr Biochem*. 2009;20:663–76.
- Nemeth JA, Yousif R, Herzog M, Che M, Upadhyay J, Shekarriz B, et al. Matrix metalloproteinase activity, bone matrix turnover, and tumor cell proliferation in prostate cancer bone metastasis. *J Natl Cancer Inst*. 2002;94:17–25.
- Burg-Roderfeld M, Roderfeld M, Wagner S, Henkel C, Grotzinger J, Roeb E. MMP-9-hemopexin domain hampers adhesion and migration of colorectal cancer cells. *Int J Oncol*. 2007;30:985–92.
- Denizot F, Lang R. Rapid colorimetric assay for cell growth and survival. Modifications to the tetrazolium dye procedure giving improved sensitivity and reliability. *J Immunol Methods*. 1986;89:271–7.
- Ruiz Y, Rodrigues J, Arvelo F, Usabillaga A, Monsalve M, Diez N, et al. Cytotoxic and apoptosis-inducing effect of ent-15-oxokaur-16-en-19-oic acid, a derivative of grandiflorolic acid from *Espeletia schultzei*. *Phytochemistry*. 2008;69:432–8.
- Atienza JM, Zhu J, Wang X, Xu X, Abassi Y. Dynamic monitoring of cell adhesion and spreading on microelectronic sensor arrays. *J Biomol Screen*. 2005;10:795–805.
- Rodriguez LG, Wu X, Guan JL. Wound-healing assay. *Meth Mol Biol*. 2005;294:23–9.
- Powell AA, Akare S, Qi W, Herzer P, Jean-Louis S, Feldman RA, et al. Resistance to ursodeoxycholic acid-induced growth arrest can also result in resistance to deoxycholic acid-induced apoptosis and increased tumorigenicity. *BMC Cancer*. 2006;6:219.
- Qu X, Yuan Y, Xu W, Chen M, Cui S, Meng H, et al. Caffeoyl pyrrolidine derivative LY52 inhibits tumor invasion and metastasis via suppression of matrix metalloproteinase activity. *Anticancer Res*. 2006;26:3573–8.
- Ribatti D, Gualandris A, Bastaki M, Vacca A, Iurlaro M, Roncali L, et al. New model for the study of angiogenesis and antiangiogenesis in the chick embryo chorioallantoic membrane: the gelatin sponge/chorioallantoic membrane assay. *J Vasc Res*. 1997;34:455–63.
- Feldman JP, Goldwasser R, Mark S, Schwartz J, Orion I. A mathematical model for tumor volume evaluation using two-dimensions. *J Appl Quant Meth*. 2009;4:455–62.

21. Kumar B, Koul S, Khandrika L, Meacham RB, Koul HK. Oxidative stress is inherent in prostate cancer cells and is required for aggressive phenotype. *Cancer Res.* 2008;68:1777–85.
22. Freedman VH, Shin SI. Cellular tumorigenicity in nude mice: correlation with cell growth in semi-solid medium. *Cell.* 1974;3:355–9.
23. Boumendjel A, Boccard J, Carrupt PA, Nicolle E, Blanc M, Geze A, *et al.* Antimitotic and antiproliferative activities of chalcones: forward structure-activity relationship. *J Med Chem.* 2008;51:2307–10.
24. Nishimura R, Tabata K, Arakawa M, Ito Y, Kimura Y, Akihisa T, *et al.* Isobavachalcone, a chalcone constituent of *Angelica keiskei*, induces apoptosis in neuroblastoma. *Biol Pharm Bull.* 2007;30:1878–83.
25. Saxena HO, Faridi U, Kumar JK, Luqman S, Darokar MP, Shanker K, *et al.* Synthesis of chalcone derivatives on steroidal framework and their anticancer activities. *Steroids.* 2007;72:892–900.
26. Lee YS, Lim SS, Shin KH, Kim YS, Ohuchi K, Jung SH. Anti-angiogenic and anti-tumor activities of 2'-hydroxy-4'-methoxy-chalcone. *Biol Pharm Bull.* 2006;29:1028–31.
27. Motani K, Tabata K, Kimura Y, Okano S, Shibata Y, Abiko Y, *et al.* Proteomic analysis of apoptosis induced by xanthoangelol, a major constituent of *Angelica keiskei*, in neuroblastoma. *Biol Pharm Bull.* 2008;31:618–26.
28. Zhou J, Geng G, Batist G, Wu JH. Syntheses and potential anti-prostate cancer activities of ionone-based chalcones. *Bioorg Med Chem Lett.* 2009;19:1183–6.
29. Pilatova M, Varinska L, Perjesi P, Sarissky M, Mirossay L, Solar P, *et al.* *In vitro* antiproliferative and antiangiogenic effects of synthetic chalcone analogues. *Toxicol in vitro.* 2010;24:1347–55.
30. Ding L, Liu B, Qi LL, Zhou QY, Hou Q, Li J, *et al.* Antiproliferation, cell cycle arrest and apoptosis induced by a natural xanthone from *Gentianopsis paludosa* Ma, in human promyelocytic leukemia cell line HL-60 cells. *Toxicol in vitro.* 2009;23:408–17.
31. Kamal A, Ramakrishna G, Raju P, Viswanath A, Janaki RM, Balakishan G *et al.* Synthesis and anti-cancer activity of chalcone linked imidazolones. *Bioorg Med Chem Lett.* 2010;Epub ahead of print, June 25;doi:10.1016/j.bmcl.2010.06.097.
32. Lee YM, Lim DY, Choi HJ, Jung JI, Chung WY, Park JH. Induction of cell cycle arrest in prostate cancer cells by the dietary compound isoliquiritigenin. *J Med Food.* 2009;12:8–14.
33. Liotta LA, Stetler-Stevenson WG. Principles of molecular cell biology of cancer metastasis. In: De Vita VT, Hellman S, Rosenberg SA, editors. *Cancer: principles and practice oncology.* Philadelphia: Lippincott; 1993. p. 134–49.
34. McCawley LJ, Matrisian LM. Matrix metalloproteinases: they're not just for matrix anymore! *Curr Opin Cell Biol.* 2001;13:534–40.
35. Papi A, Bartolini G, Ammar K, Guerra F, Ferreri AM, Rocchi P, *et al.* Inhibitory effects of retinoic acid and IIF on growth, migration and invasiveness in the U87MG human glioblastoma cell line. *Oncol Rep.* 2007;18:1015–21.
36. Sava G, Zorzet S, Turrin C, Vita F, Soranzo M, Zabucchi G, *et al.* Dual Action of NAMI-A in inhibition of solid tumor metastasis: selective targeting of metastatic cells and binding to collagen. *Clin Cancer Res.* 2003;9:1898–905.
37. Fisher C, Gilbertson-Beadling S, Powers EA, Petzold G, Poorman R, Mitchell MA. Interstitial collagenase is required for angiogenesis *in vitro.* *Dev Biol.* 1994;162:499–510.
38. Zhu XF, Xie BF, Zhou JM, Feng GK, Liu ZC, Wei XY, *et al.* Blockade of vascular endothelial growth factor receptor signal pathway and antitumor activity of ON-III (2', 4'-dihydroxy-6'-methoxy-3', 5'-dimethylchalcone), a component from Chinese herbal medicine. *Mol Pharmacol.* 2005;67:1444–50.
39. Bhoopathi P, Chetty C, Gujrati M, Dinh DH, Rao JS, Lakka SS. The role of MMP-9 in the anti-angiogenic effect of secreted protein acidic and rich in cysteine. *Br J Cancer.* 2010;102:530–40.
40. Eliceiri BP, Cheresh DA. Adhesion events in angiogenesis. *Curr Opin Cell Biol.* 2001;13:563–8.
41. Hynes RO. A reevaluation of integrins as regulators of angiogenesis. *Nat Med.* 2002;8:918–21.
42. Cifone MA, Fidler IJ. Correlation of patterns of anchorage-independent growth with *in vivo* behavior of cells from a murine fibrosarcoma. *Proc Natl Acad Sci USA.* 1980;77:1039–43.
43. Petrelli A, Valabrega G. Multitarget drugs: the present and the future of cancer therapy. *Expert Opin Pharmacother.* 2009;10:589–600.